Astron. Astrophys. 353, 1083–1093 (2000)

ASTRONOMY AND ASTROPHYSICS

EUV brightness variations in the quiet Sun

A. Brković[1], I. Rüedi[2], S.K. Solanki[3], A. Fludra[4], R.A. Harrison[4], M.C.E. Huber[5], J.O. Stenflo[1], and K. Stucki[1]

[1] Institute of Astronomy, ETH-Zentrum, 8092 Zürich, Switzerland
[2] Physikalisch-Meteorologisches Observatorium Davos, World Radiation Center, 7260 Davos Dorf, Switzerland
[3] Max-Planck-Institut für Aeronomie, Max-Planck-Strasse 2, 37191 Katlenburg-Lindau, Germany
[4] Space Science Department, Rutherford Appleton Laboratory, Chilton, Didcot, Oxfordshire OX11 0QX, UK
[5] ESA, Space Science Deptartment, ESTEC, PO Box 299, 2200 AG Noordwijk, The Netherlands

Received 16 July 1999 / Accepted 18 October 1999

Abstract. The Coronal Diagnostic Spectrometer (CDS) onboard the SOHO satellite has been used to obtain movies of quiet Sun regions at disc centre. These movies were used to study brightness variations of solar features at three different temperatures sampled simultaneously in the chromospheric He I 584.3 Å ($2{\cdot}10^4$ K), the transition region O V 629.7 Å ($2.5{\cdot}10^5$ K) and coronal Mg IX 368.1 Å (10^6 K) lines.

In all parts of the quiet Sun, from darkest intranetwork to brightest network, we find significant variability in the He I and O V line, while the variability in the Mg IX line is more marginal. The relative variability, defined by rms of intensity normalised to the local intensity, is independent of brightness and strongest in the transition region line. Thus the relative variability is the same in the network and the intranetwork. More than half of the points on the solar surface show a relative variability, determined over a period of 4 hours, greater than 15.5% for the O V line, but only 5% of the points exhibit a variability above 25%. Most of the variability appears to take place on time-scales between 5 and 80 minutes for the He I and O V lines.

Clear signs of "high variability" events are found. For these events the variability as a function of time seen in the different lines shows a good correlation. The correlation is higher for more variable events. These events coincide with the (time averaged) brightest points on the solar surface, i.e. they occur in the network. The spatial positions of the most variable points are identical in all the lines.

Key words: Sun: chromosphere – Sun: corona – Sun: transition region – Sun: UV radiation

1. Introduction

The variability of the Sun's upper atmosphere on time scales less than a day has been studied using a variety of instruments. Early work used instruments on the Skylab mission (e.g. Rabin & Dowdy 1992, in the quiet Sun) and the Solar Maximum Mission (SMM, e.g. Porter et al. 1984, in an active region). In spite of suffering from poor spatial sampling these instruments revealed intriguing insights. Thus Porter et al. (1984) discovered transition region brightenings lasting typically less than 1 minute, while Rabin & Dowdy (1992) reported on transition region brightenings lasting longer than 5 minutes and found that most of the significant fluctuations last for ≤ 10 minutes, though a non-negligible amount of points shows longer lasting brightenings. Lites & Hansen (1977) analysed images of solar active regions using *OSO-8* data and reported on transient brightenings of transition region lines of up to factors of 10 lasting several minutes and showing a repetitive character.

The improved performance of the instruments onboard of the Solar and Heliopsheric Observatory (SOHO) and Yohkoh satellites allow this topic to be investigated in greater detail. Strong et al. (1992) used the Soft X-ray Telescope (SXT) onboard Yohkoh to study X-ray bright points (XBPs). They found that the longer-lived XBPs exhibit significant intensity fluctuations on time-scales from a few minutes to hours. Shimizu et al. (1992) reported that transient brightenings were typically observed at a rate of one every 3 min in very active regions, down to one every hour in somewhat quieter active regions. Berghmans et al. (1998) studied quiet Sun EUV transient brightenings by applying a Fourier analysis to data obtained with the Extreme-Ultraviolet Imaging Telescope (EIT) onboard SOHO, and reported that transition region brightenings last from 2 to 60 min, while brightenings in the low corona range from 2 to 30 min. Finally, strong transient brightenings called blinkers have been observed on a time-scale of tens of minutes in the quiet Sun (Harrison 1997) and in active regions (Walsh et al. 1997) using CDS on SOHO.

The study of solar variability could provide clues for understanding how the solar chromosphere, transition-region and corona are heated, since heating events, be they due to magnetic reconnection or the dissipation of wave pulses, are expected to produce transient brightenings in the emission from the relevant atmospheric layers (e.g. Schadee et al. 1983; Lin et al. 1984, Parker 1987, Ulmschneider et al. 1991).

In this paper we present the results of a statistical analysis of the brightness variations observed in the quiet Sun using movies, obtained with the Coronal Diagnostic Spectrometer (CDS). A

Send offprint requests to: brkovic@astro.phys.ethz.ch

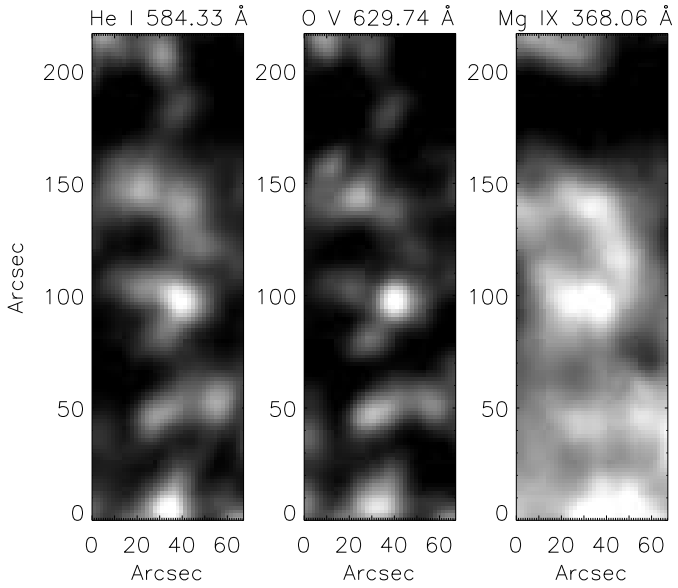

Fig. 1. A time-averaged quiet-Sun CDS movie frame recorded on 3rd December 1996. From left to right: He I 584 Å, O V 629 Å and Mg IX 368 Å. The field of view corresponds to $67'' \times 217''$. Brighter areas correspond to higher intensities.

preliminary version of some of the results was presented by Rüedi et al. (1997).

2. Observations

The analysed observations have been carried out using the Normal Incidence Spectrometer (NIS) of CDS (Harrison et al. 1995) in its movie mode, i.e. with the $90'' \times 240''$ slit. In this mode a filtergram covering a part of the solar surface corresponding to the slit size is produced at each wavelength. Filtergrams in 3 strong and sufficiently isolated spectral lines, He I 584.3 Å ($2{\cdot}10^4$ K), O V 629.7 Å ($2.5{\cdot}10^5$ K) and Mg IX 368.1 Å (10^6 K), were recorded simultaneously. Spectral information within each spectral line is lost. The images were obtained at a cadence of 31 seconds for a duration of 4 hours each on 3rd December 1996 and on 6th December 1996. The actual exposure time was 25 seconds and the overhead per frame amounted to 6 seconds (the overhead is mainly for reading out the CCD and preparing it ready for the next exposure). The targets were quiet regions at the centre of the solar disc. Fig. 1 shows a time-averaged frame in each spectral line. The panels correspond from left-to-right to the He I 584 Å, O V 629 Å and Mg IX 368 Å lines.

After carrying out the standard reduction procedure - i.e., correcting for bias of detector, calibration, etc.- we used cross-correlations and pointing information provided by the instrument housekeeping data to compensate for solar rotation and changes in the telescope pointing. Therefore, in the reduced time series, each pixel follows the same point on the solar surface during the whole time series. The size of the resulting field of view is $67'' \times 217''$ (40×129) pixels, with the pixel size being $1.68'' \times 1.68''$. We took special care to interpolate over pixels with missing data and pixels contaminated by cosmic rays. Finally, the data were corrected, to first order, for the slow evolution of the geometrical structure of solar features by removing the long-term linear trend. This was done separately for each pixel and spectral line.

We quantify the variability through the rms of the time series. Due to the broad point-spread-function of CDS individual pixels are not independent in their brightness or noise properties. If analysed individually normal statistics could then not be applied to determine the photon noise ($\sqrt{\text{Intensity}}$). Thus we found that the variability determined from individual pixels in the Mg IX line is far smaller than the photon noise, if the later is simply determined using the data from that pixel. To resolve this problem we bin the intensities from groups of 4x4 pixels for most of the analysis described here. This is the minimum binning required in order to achieve nearly critical sampling (compare with the point spread functions given by Harrison et al. 1995 and Pauluhn et al. 1999). In this manner the S/N ratio is increased by a factor of 4 and, as we shall see in Sect. 3.2, the variability of the Mg IX line appears marginally significant. Note that, following Thompson (1998) the noise has been multiplied by $\sqrt{2}$. The binning over 16 pixels is a compromise: averaging over more pixels improves the statistics somewhat, but decreases the number of individually analysed spatial pixels.

The average S/N ratios, after grouping 4x4 pixels, are 65.4 and 70.3 for He I, 44.9 and 49.2 for O V and 26.4 and 25.9 for Mg IX for the two data sets, respectively. In the following we analyse the temporal intensity variations for each of the 320 binned pixels.

3. Results

3.1. Intensity distribution

Intensity distributions in EUV lines (originating from the upper chromosphere to the corona) of the quiet Sun are given by Huber et al. (1974) and Reeves et al. (1976), based on *Skylab* data, by Lemaire et al. (1997) who used the Solar Ultraviolet Measurements of Emitted Radiation (SUMER) spectrograph onboard SOHO, and by Gallagher et al. (1998), from CDS scans. According to the first three of these investigations the distributions in the quiet Sun can be characterized by a peak at a relatively low intensity and a high-intensity tail. Gallagher et al. (1998) showed that the intensity histograms of 10 spectral lines (originating from the upper chromosphere to the corona) can be described by the sum of two Gaussians.

Histograms of the temporally averaged intensity obtained from our data are displayed in Fig. 2. The distributions of the intensity in He I (solid curves) and O V lines (dash-dotted curves) have a peak at a relatively low intensity and a high-intensity tail in both data sets, while they are rather narrow in the Mg IX line (dashed curves). The tail of high intensity points seen in He I and O V is due to the high contrast of the network in these lines (the bright features in the left and middle panels of Fig. 1). This network is still recognizable in the images recorded in the Mg IX line, but at a much lower contrast, and covering a larger fraction of the solar surface, which leads to the narrower and more symmetric histograms of this line. In the first data set the

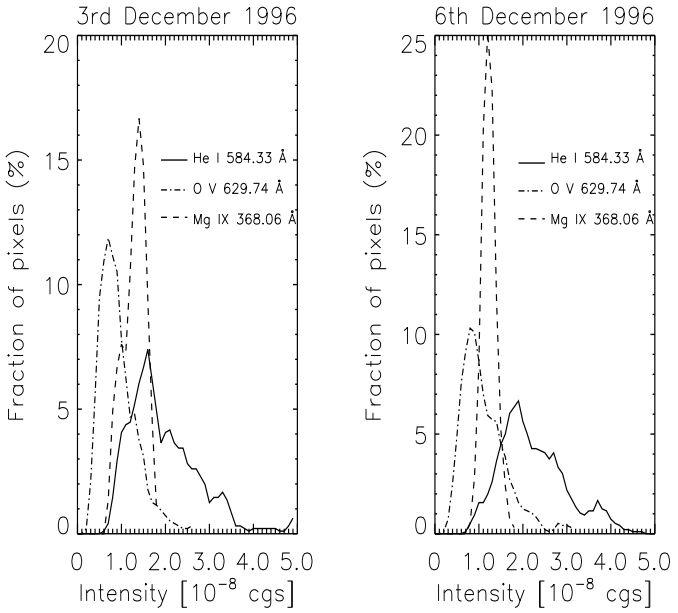

Fig. 2. Histograms of the intensity values recorded in the 3 spectral lines. The intensity is given in cgs units, i.e. in ergs/cm^2/arcsec^2/sec.

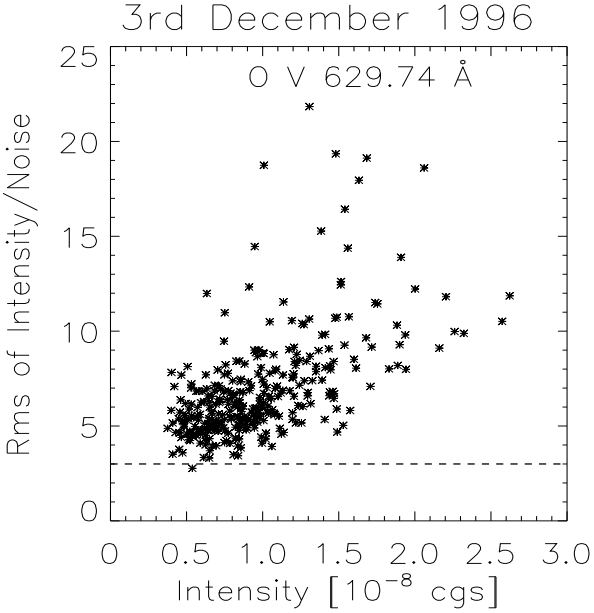

Fig. 3. Scatter plot of the ratio of the intensity-rms to the noise of the O V line at 629 Å as a function of its intensity. The horizontal dashed line represents rms values corresponding to the 3σ noise level.

distribution in the Mg IX line is slightly broader than in the second data set and shows hints of a second peak. This line is actually a blend of a Mg IX (10^6 K) and a Mg VII ($6 \cdot 10^5$ K) lines (Brekke et al. 1997). Using the CHIANTI database (Dere et al. 1997, Landi et al. 1999) we find that the expected relative strengths of the Mg VII line to the Mg IX line is 0.25 in the quiet Sun. This blending is unlikely to be responsible for the double-peaked distribution because the second data set exhibits a single-peaked distribution, while Gallagher et al. (1998) also observed a double-peaked distribution in the unblended Mg X 624.95 Å line. The 2 peaks are characteristic of the solar features present at the observed location.

3.2. Reality of the brightness variations

To judge the reality of the brightness variations with time we first determined and plotted the ratio of the rms intensity fluctuations to the noise as a function of the intensity for each of the 320 binned pixels. This is shown on Fig. 3 for the O V line. The rms is computed over the whole duration of the observations (4 hours). The noise and the intensity are averages over this period of time.

Since all but one of the points lie above an rms/noise ratio of 3.0 all intensity variations are larger than the noise and consequently real. Significant variabilities are observed at all intensities. The possibility that the geometrical evolution of the brightness structures produces a substantial amount of these variabilities was tested by removing a long-term linear trend for each pixel. No significant changes in the plot were noticed before and after this correction (all the results presented in this paper were obtained after the removal of such trends). The overall shape of the corresponding plot for the He I line is similar to Fig. 3, with a somewhat higher S/N ratio and only marginally lower rms/noise.

We tested to see if pointing errors due to the jitter of the spacecraft and the instrument could produce the observed variations by making a Monte–Carlo simulation. Pre-launch tests give a value of below $0.1''$ for the spacecraft jitter, while the CDS instrument itself is expected to be even more stable. We therefore produced 120 pairs of normally-distributed random numbers, corresponding to shifts in the x and y directions (along and across the slit, respectively) with a standard deviation of $0.15''$. We selected arbitrary frames for each spectral line and shifted these frames according to the values of the "Monte–Carlo" shifts, thus creating artificial time-series in which the variability is produced solely by the jitter of the spacecraft. The analysis of these time-series reveals that the jitter can contribute to at the most 10% of the observed variations. Hence most of the observed fluctuations are intrinsic variations of the solar radiation.

Fig. 4 shows the percentage of pixels with an rms/noise ratio lying above the corresponding value on the abscissa. For each spectral line two curves are plotted, corresponding to the two analysed data sets (of 3rd December 1996 and 6th December 1996, respectively). The difference between the two days is not significant. The vertical dashed line marks rms values corresponding to the 1σ noise level. The most significant variations are observed in the O V line, while the Mg IX line shows the least significant, barely marginal variations. Recall that the noise level depends on the amount of binning. The rms of the intensity, however, is almost identical for single pixels and the 4x4 binned pixels, as is expected as long as the spatial resolution element of CDS is not smaller than the binned pixel. Since the true variability cannot be smaller than the noise, the

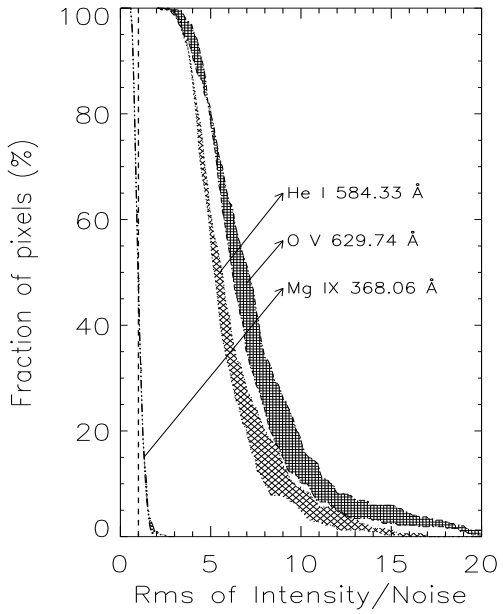

Fig. 4. Fraction of points with an intensity-rms/noise ratio lying above the corresponding value on the abscissa. For each spectral line the shaded region is enclosed by two curves resulting from the two analysed data sets. The vertical dashed line marks rms values corresponding to the 1σ noise level.

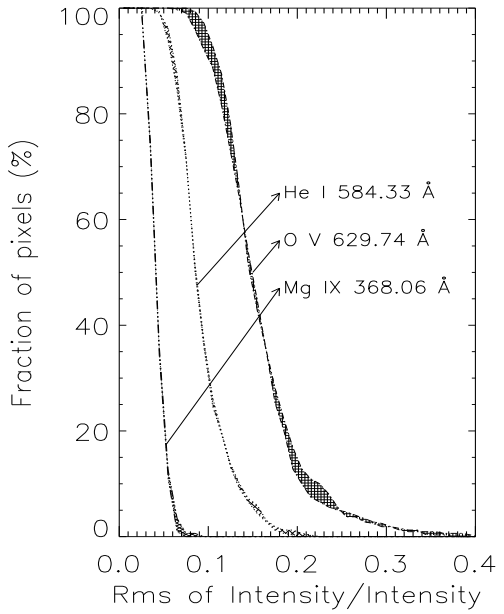

Fig. 5. Fraction of points with relative variability lying above the corresponding value on the abscissa. The two curves for each spectral line were obtained from the two analysed data sets.

rms/noise ratios plotted in Figs. 3 and 4 are lower limits. Fig. 4 tells us that basically every point in the quiet Sun is significantly variable at the 1σ level in the upper chromospheric and transition region lines (in agreement with Rabin & Dowdy 1992 and Berghmans et al. 1998). Only 47% of the points of the coronal line are significantly variable at the 1σ level (for the 4x4 binned data, which are analysed here), but, as mentioned above, this proportion depends on the amount of binning.

The difference in the significance of the variability exhibited by the 3 lines is not due to different noise levels, but rather to absolute differences in variability. This is illustrated by Fig. 5, which is similar to Fig. 4, but with the difference that the abscissa is the relative variability (i.e. rms/intensity) instead of rms/noise. The highest relative variability is observed in the O V line, followed by the He I line, with the least being in the Mg IX line. The median variability for the 3 spectral lines is found to be 15.5% for the O V line, 8.5% for the He I line and 3.5% for the Mg IX line.

Let us now test whether the variability shown by Mg IX is really due to noise, as suggested by Fig. 4, or if at least a part of it is real. To this end we plot pixel-by-pixel the variability in one line vs. the variability in another line (Fig. 6). Prior to plotting we collected the data points into bins of 32 points each according to their variability in the spectral line. I.e., we first take the 32 points with the lowest variability values on the abscissa and find their average value. Then, for the spectral line on the ordinate we take the 32 corresponding values of rms and determine their average value and standard deviation. Then, we proceed with the next 32 points and so on. The binned variability is represented by the solid line, the standard deviation by the dotted lines. The curves show a significant inclination, implying that the variability in one line is related to the variability in another line. The correlation coefficients between the variabilities support this and amount to 0.77 and 0.86 for the O V–He I pair, 0.53 and 0.65 for the Mg IX–He I pair and 0.45 and 0.64 for the Mg IX–O V pair. The correlation coefficients were determined using all the 320 points, i.e., prior to this second round of binning. The correlation between the Mg IX line and the two other lines implies that at least some of the variability seen in the Mg IX line is of solar origin. Since according to Fig. 4 the variability of the Mg IX line is barely significant, Fig. 6 indicates that the noise estimate is still somewhat too large, even after binning. Not surprisingly, the correlation is largest between He I and O V, but it is slightly larger between He I and Mg IX than between O V and Mg IX. This may at first sight appear surprising since the O V lines samples a temperature between He I and Mg IX, so that variability that takes place simultaneously at the chromospheric and coronal levels should also be visible in between. The solution to this riddle may well lie in the complex formation of the He I line, which is also somewhat sensitive to coronal properties (Fontenla et al. 1993; Andretta & Jones 1997). Hence, the large correlation between He I and Mg IX may simply reflect the fact that a part of the fluctuations seen in He I are actually coronal in origin. Since the coronal radiation is far less variable than the transition region radiation (as suggested by the Mg IX and O V curves in Fig. 5) the lower relative variability of the He I line (i.e. variability over intensity) must not on its own signify that chromospheric radiation is less variable. The argument for that chromospheric radiation is less variable could be in the results of Rabin & Dowdy (1992) who found that the relative variability in the chromospheric H I Ly α line is smaller than in any of the transition region lines

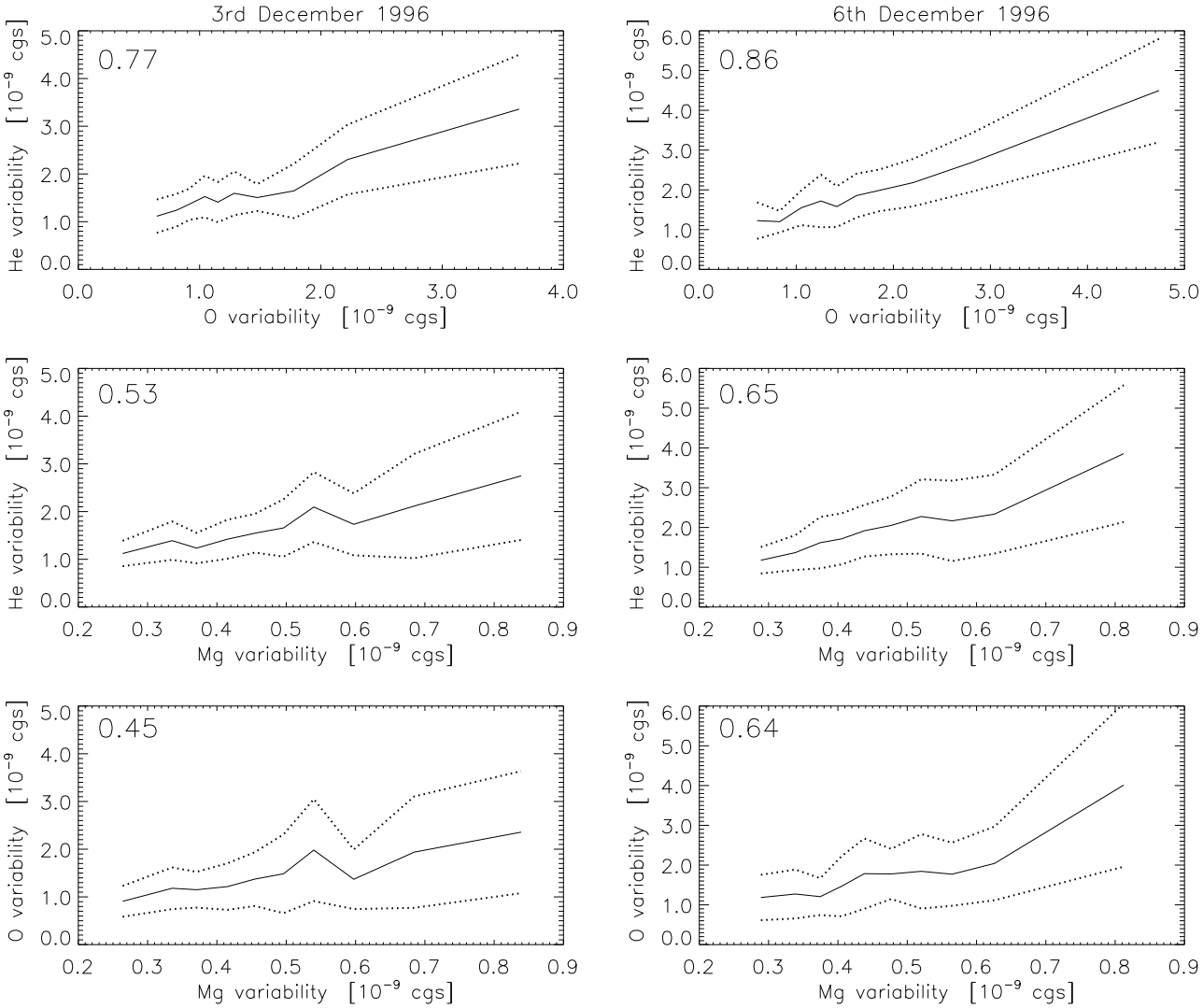

Fig. 6. Variability exhibited by one spectral line vs. variability of another line. Solid curves: binned values (see text for details). Dotted curves indicate the 1σ uncertainties. The correlation coefficient between two variabilities is given at the upper left corner of each frame. Left-hand frames: data obtained on 3rd December 1996, right-hand frames: data obtained on 6th December 1996.

they observed. The non-negligible correlation between the O V and the Mg IX variability is in agreement with the finding of Berghmans et al. (1998) of the similarity between the parameters characterising brightenings detected in lines formed in the transition region and cooler parts of the corona. This suggests that the brightenings in both layers result from the same physical processes.

3.3. Relative intensity fluctuations

Fig. 7 shows binned values of the relative intensity fluctuations of each spectral line as a function of the time-averaged intensity (solid lines). Prior to plotting the data from all 320 pixels, the points were combined according to increasing intensity into 10 bins, each containing 32 points. The dotted lines indicate the standard deviation of the points in the bin. The relative variability does not depend on intensity, within the uncertainties. The small correlation coefficients between the relative intensity fluctuations and the intensity (also indicated on the plots), amounting to -0.21 and 0.03 for He I, 0.10 and 0.29 for O V, and 0.17 and 0.24 for Mg IX, confirm that the *relative* intensity variations do not depend significantly on the absolute intensity in a spectral feature, irrespective of the spectral line, i.e. of the temperature. This result implies that the relative brightness fluctuations are equally strong in the network as in the intranetwork. Vernazza et al. (1975) found the same result for the chromospheric and transition region EUV lines they used. The average values of the relative intensity fluctuations are identical for the two data sets and amount to 8.8% for He I, 15.2% for O V and 3.7% for Mg IX (the averaging was done over all 320 values). These values are compatible with those of Berghmans et al. (1998), who got 16% for the He II 304 Å line and 5% for the Fe XII 195 Å coronal line.

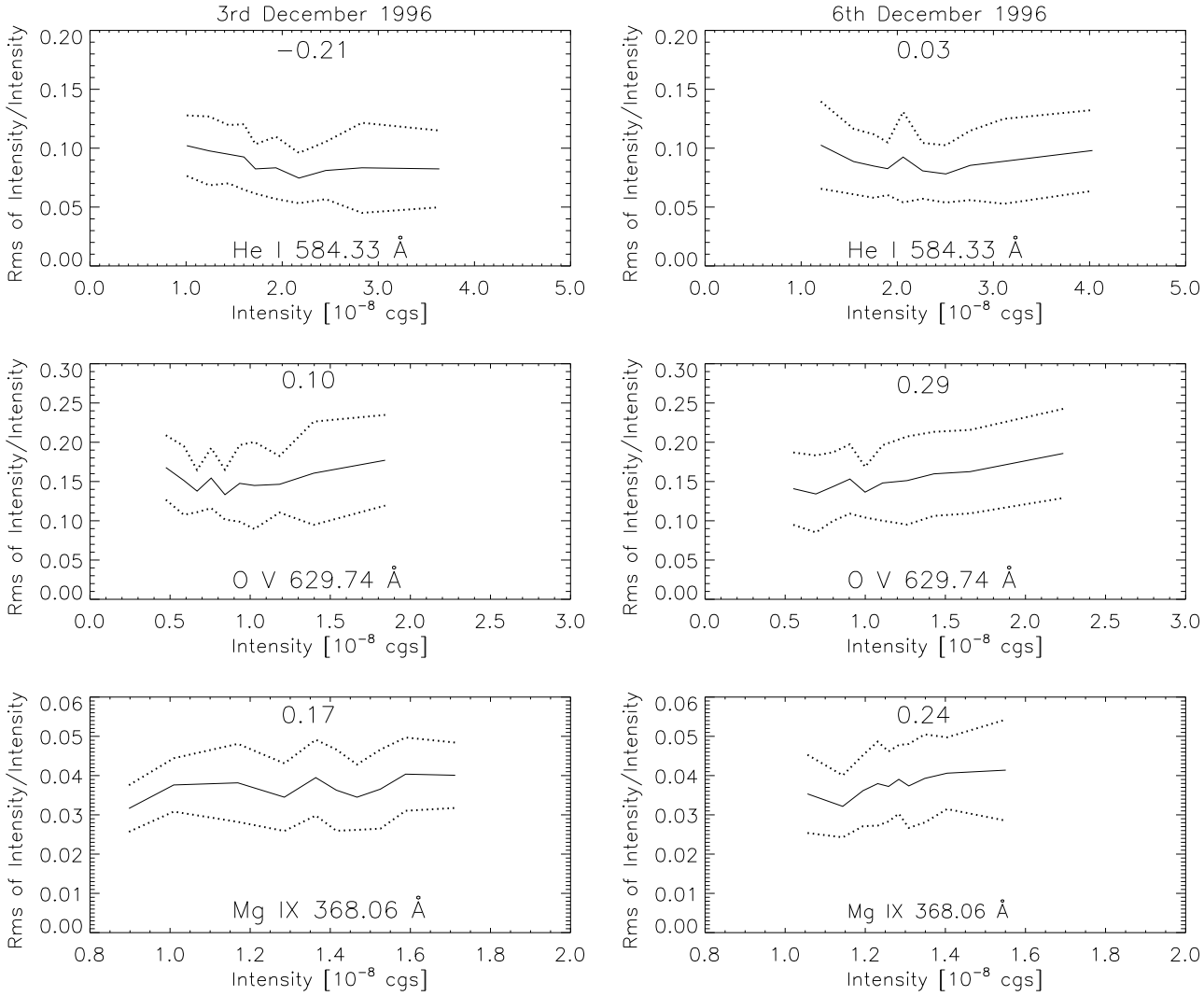

Fig. 7. Relative intensity fluctuations (rms of intensity/intensity) vs. intensity for each spectral line (from top to bottom) and for the two days (left: 3rd December 1996, right: 6th December 1996). Solid curves: values binned over 32 points with neighbouring intensities. The dotted curves indicate the standard deviation. The correlation coefficient between relative intensity fluctuations and intensity is given at the top of each frame.

The correlation seen in Fig. 6 between different spectral lines may to some extent reflect the approximately linear dependence of absolute variability on brightness valid for each line implied by Fig. 7 (recall that the time-averaged brightness is correlated from one line to the next; see Fig. 1).

Next we investigate, in a very simple manner, the time scales of the variability seen in our data set. In order to determine the relative brightness fluctuations occurring over time-scales of 5 minutes or less (or 80 minutes or less), we cut our 4 hour sequence into 5 (or 80) minute pieces. For each of these we determine the rms of the intensity for each binned pixel separately. For the relative brightness fluctuations occurring on time-scales between 5 minutes and 4 hours we determined the average intensity observed in each 5 minute interval. The standard deviation of these values represents the brightness fluctuations on time-scales larger than 5 minutes for a given pixel.

Fig. 8 shows histograms of the relative intensity fluctuations on different time-scales (as indicated in the figure). It displays the percentage of pixels with a relative intensity fluctuation value corresponding to the value on the abscissa. The relative intensity fluctuations observed over short time-scales (i.e. ≤ 5 min, thin solid curves) are much smaller than the fluctuations observed over the 3 other time-scales (i.e., fluctuations on time-scales ≥ 5 min and ≤ 240 min, on time-scales of ≤ 80 min and on time-scale of ≤ 240 min). To test the significance of these histograms we created an artificial data set consisting of 2x320 time series with the same averaged intensities as the observations, but with fluctuations due purely to white noise with an amplitude corresponding to that expected for photon noise. A comparison between these artificial histograms and the observed ones reveals that for He I and O V all fluctuations except those shorter than 5 min are almost entirely unaffected by noise. Even the short fluctuations are partly (He I) or largely (O V) solar.

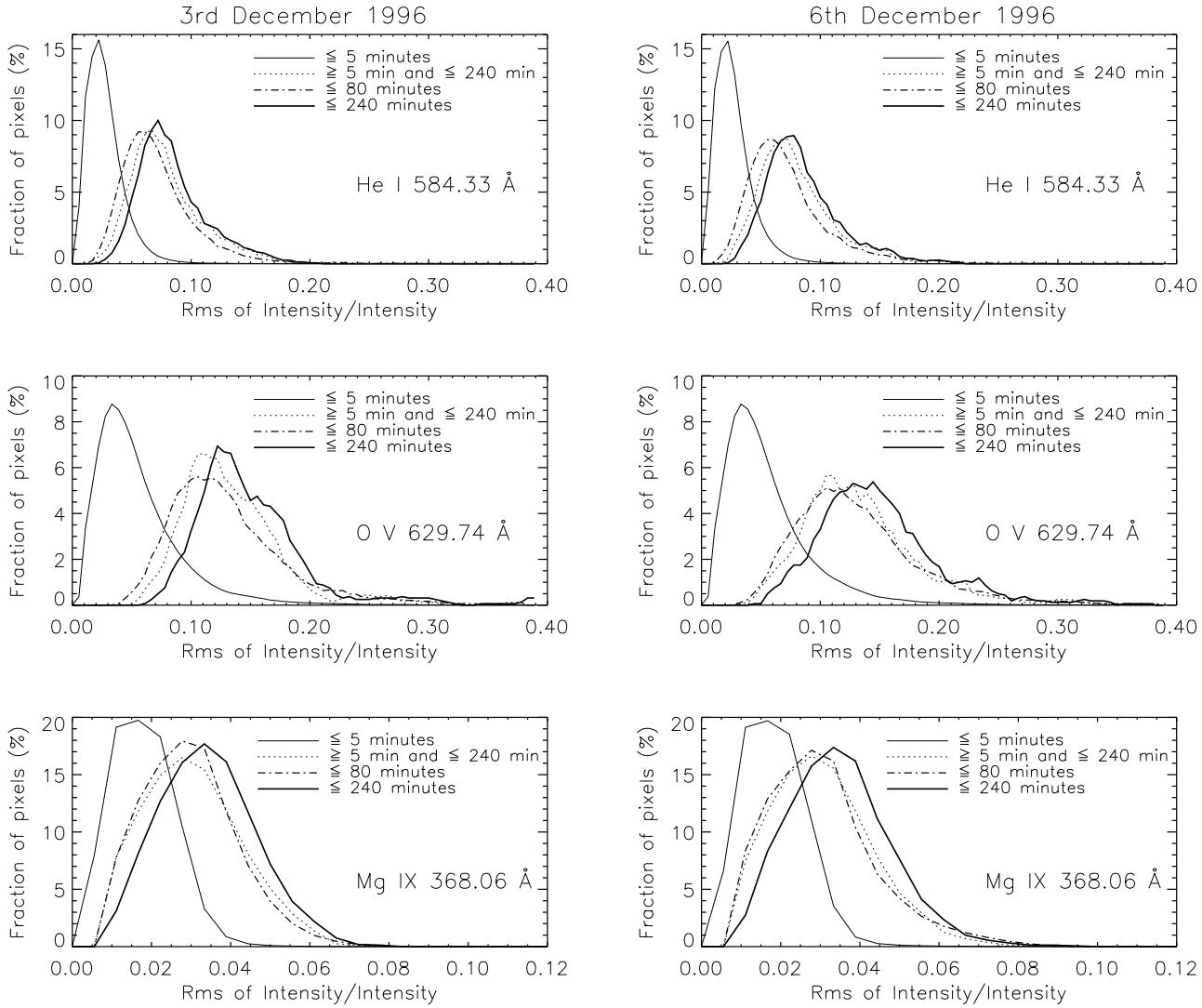

Fig. 8. Histograms of relative intensity fluctuations. The thin solid lines correspond to variations with time-scales shorter than 5 minutes, the dashed curves to variations with time-scales longer than 5 minutes, the dash-dotted curves to variations with time-scales shorter than 80 minutes and the thick solid lines to all variations with time-scales below 240 minutes (i.e. the full period of 4 hours).

Since we are probably overestimating the noise (see Sect. 3.2 and below) we expect that for both these lines most of the short variations are real. In the case of Mg IX the noise histograms for the variations $\leq$ 80 min and $\leq$ 240 min are similar to the observed ones, the observed variations $\geq$ 5 min possess a larger amplitude than the noise, while the observed fluctuations $\leq$ 5 min lie below the noise. This confirms that we are still overestimating the noise somewhat. Scaling it in such a way that the short Mg IX fluctuations are compatible with noise suggests that the Mg IX fluctuations $\geq$ 5 min are almost entirely solar. From the similarity of all plotted curves except that for fluctuations shorter than 5 min, as well as from a similar histogram for fluctuations between 5 and 80 minutes we conclude that the brightness fluctuations occurr dominantly on time-scale between 5 and 80 minutes.

For all the time-scales investigated the transition region line exhibits the largest variability while the coronal line is least variable (in agreement with Vernazza et al. 1975). The apparent tendency for the Mg IX line to show more rapid fluctuations may well have to do with the lower significance of the variability of this line, so that this result should be considered with some caution.

3.4. Analysis of "high variability" events

The Figs. 9a–f show scatter-plots of the absolute variability of the O V line over 5 minutes against the intensity for six consecutive 5 minutes intervals. During this period of half an hour, the variability of some points changed dramatically, first increasing and then decreasing. In panels b–e a significant number of pixels shows a much larger variability than average, larger even than the maximum reached at other times (compare with frames a and f). We concentrate here on the most variable pixels and consider single pixels (i.e. without the 4x4 binning). We there-

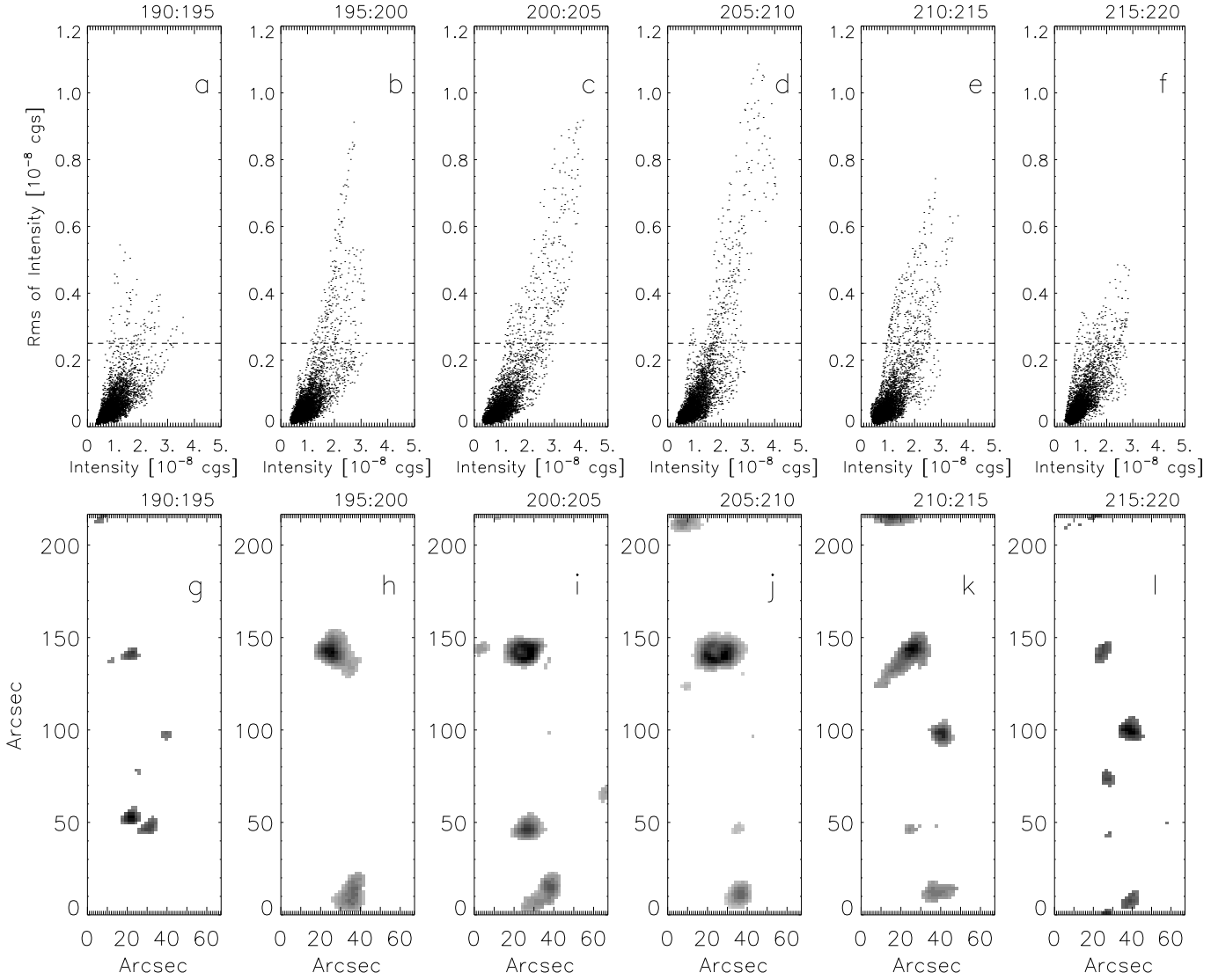

Fig. 9. Scatter-plots of the (absolute) variability vs. the intensity (frames a–f, upper row) and spatial images showing the points with variability $\geq 2.5\times10^{-9}$ cgs (frames g–l, lower row) for 6 consecutive 5-minute intervals. The time ranges (in minutes since the start of the observations) are given at the top of each plot. The dataset is of 3rd December 1996 for the O V line. Darker shading in the lower row (panels g–l) corresponds to higher variability.

fore selected the pixels with variability in the O V line $\geq 2.5\times 10^{-9}$ cgs in any given 5 minute interval. In Figs. 9a–f this threshold is marked by the horizontal dashed line. On average, 2.0% of the pixels fulfill this condition. For the data shown in Fig. 9 these percentages are 1.7, 4.4, 5.8, 5.7, 5.7 and 2.5% from left to right. The spatial locations of the pixels satisfying this condition are shaded in Figs. 9g–l. It is evident that regions of high variability are not randomly distributed but are concentrated in typically 2–5 locations within the field of view at any given time. The increase of the maximum variability and of the number of points above the threshold in Fig. 9b is due to the appearance, respectively enlargment of 2 regions of high variability. In particular the region centred approximately at ($30''$, $140''$) exhibits very intense variability. After inspecting all the spatial maps for regions having a variability at time scales $\leq$ 5 minutes above the given threshold (for the O V line), we found that over the whole 4 hours the heightened variability is concentrated in only 20 compact and spatially distinct regions in the field of view. The sizes of these 20 regions range from 5 to 30 pixels (i.e. they cover areas 14 to 85 arcsec^2). This procedure was repeated for time-scales $\leq$ 10, $\leq$ 20 and $\leq$ 40 minutes in the O V line. The regions found for these time-scales are the same as those found for the time-scale $\leq$ 5 minutes.

Note that the high-variability events which we find differ from, e.g., the blinkers (Harrison 1997) by the method used to search for them. Blinkers are brightenings which rise above a certain threshold on a time-scale of a few minutes, whereas in the events we are considering the variability is the key element. It is thus possible that although the brightness at a given point is intensely variable on a short time scale, due to repeated rapid

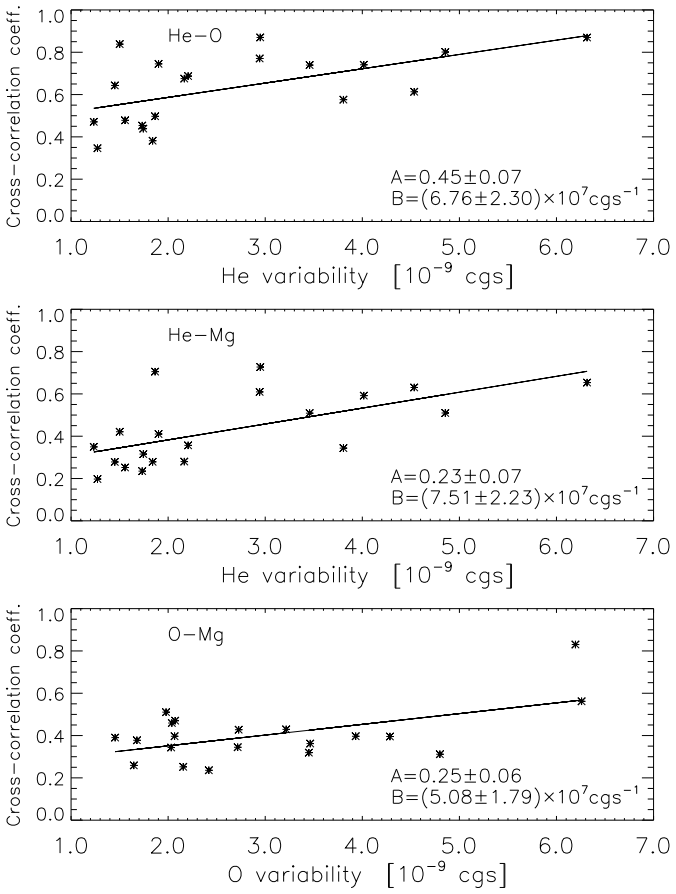

Fig. 10. Maxima of the cross-correlation coefficients between the intensity in two lines for a given region showing high variability versus the variability of the region in one of these lines. Plotted are the results for the 3rd December 1996 dataset.

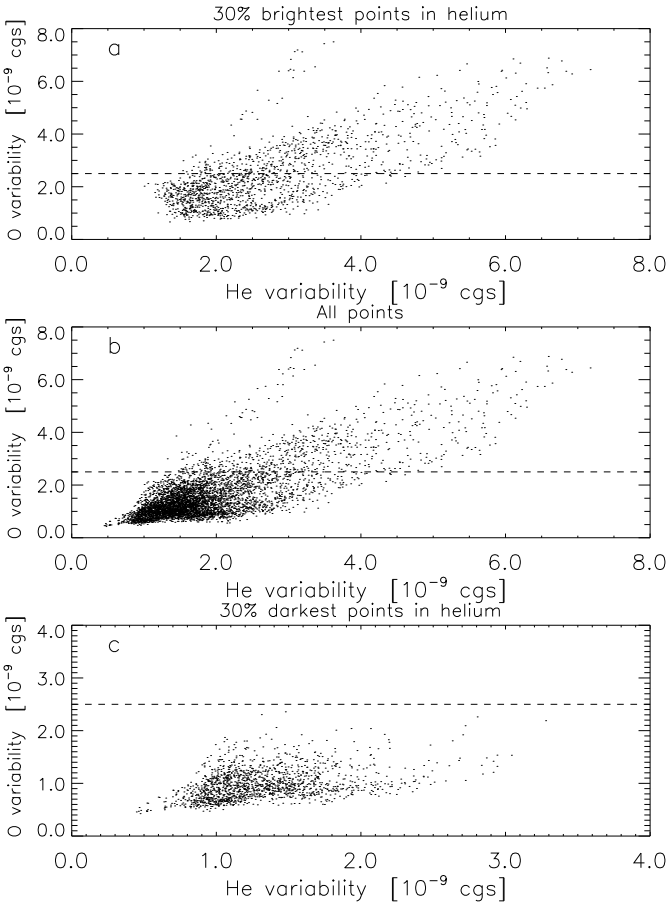

Fig. 11. Scatter-plot of the absolute variability in the He I line versus the absolute variability in the O V line for (a) 30% brightest points, (b) all points and (c) 30% darkest points in the He I line. The dataset is of 3rd December 1996.

fluctuations, it never rises above the threshold defining a blinker. We are currently identifying the blinkers in the same data sets. These are to be discussed in a separate paper in which we also intend to investigate the correspondence between blinkers and high-variability events.

At every time step we spatially averaged the intensity over the pixels belonging to a given (isolated) region of high variability. This was repeated for each of the 20 such regions, and for each spectral line. The average S/N values, for these 20 regions lie in the range 32.9–113.2 for He I, 22.7–81.0 for O V and 12.4–34.0 for Mg IX. Then, for each region we cross-correlated these time series between pairs of spectral lines. Unsurprisingly, the best cross-correlation was found between the He I and the O V line. In all but one case, the maximum of the cross-correlation coefficient was reached for zero time-lag (within an accuracy given by the exposure time of 30 seconds). The anomalous region also has second lowest cross-correlation. In other words, changes in intensity in the chromospheric and transition region lines happen simultaneously. The cross-correlation of the Mg IX line with the two other lines was of somewhat lower quality, and the correlation was not always maximum for zero time lag.

The maxima of the cross-correlation coefficients (e.g., He I–O V) are plotted as a function of the variability in He I or O V in Fig. 10. The variability, δI, is the rms taken over the full 4 hours time-series of the respective region. The plots show that regions with larger variability also exhibit a higher cross-correlation. The solid lines are linear fits between the maxima of the cross-correlation coefficients and the variabilities. The coefficients of the linear fits A + B·δI are written in the lower right corner of each plot. It is not surprising that the cross-correlations involving Mg IX depend on variability since noise is a problem with that line and the higher the variability, the less it is affected by noise. However, for He I and O V, due to the high S/N ratio, the increase of the correlation is clearly of solar origin.

We also studied how the correlation between the variability in different lines depends on brightness, by considering separately the 30% darkest and 30% brightest points of all 5160 pixels in a given spectral line. In Fig. 11 the He I and O V variabilities are plotted against each other for the brightest, the darkest and all data points. The dashed line represents the threshold value of 2.5×10^{-9} cgs explained earlier in this section. Note the axes of the panel showing the darkest points cover differ-

ent ranges, but the relative ranges of the x and y-axis are the same in all three plots. Since absolute variability increases almost linearly with brightness (see Fig. 7) it is not surprising that all darker points have a variability below the threshold value. Benz & Krucker (1998) also reported that in the quiet corona the brighter points show higher absolute variability. According to Fig. 11 the brighter and more variable points are indeed better correlated in the two lines. It is therefore in the network that variability at one temperature is most closely associated with variability at another temperature.

4. Conclusions

We have investigated the brightness variations observed in quiet Sun CDS movies obtained simultaneously in He I 584.3 Å, O V 629.7 Å and Mg IX 368.1 Å. The relative variations decrease in magnitude and significance from the O V line, over the He I line, to the Mg IX line. The average values of the relative intensity fluctuations amount to 8.8% for He I, 15.2% for O V and 3.7% for Mg IX, which is similar to the values found by Berghmans et al. (1998) who report 16% for the He II 304 Å and 5% for the Fe XII 195 Å coronal line. In the upper chromosphere and transition region over 98% of the quiet Sun area, from the darkest intranetwork to the brightest network, is significantly variable at the 3σ level. Hence all measured fluctuations are real intensity variations, in agreement with the findings of Rabin & Dowdy (1992) and Berghmans et al. (1998). In the corona at least 47% of the points show significant variability at the 1σ level. Jitter of the spacecraft or the instrument is ruled out as the cause of the observed variations.

We find that the *relative* variability is independent of the brightness at all studied temperatures. The brightness fluctuations observed in all 3 lines are dominantly due to brightness changes on time-scales less than 80 minutes and longer than 5 minutes.

Some locations on the Sun were found to be particularly variable. The most variable points in all 3 lines correspond to the same spatial locations. At these locations the variability in one line is closely related to the variability in another line and changes in intensity happen simultaneously in at least the chromosphere and transition region. The correlations between different spectral lines are better at locations which are particularly variable. Also, these correlations are better in the brighter parts of the quiet Sun, i.e. in the network.

It therefore seems that the whole upper atmosphere (i.e. chromosphere, transition region and corona, or at least its cooler parts) react together in the presence of the most violent events, while the influence of weaker events is more localised to a particular temperature regime. This statement needs to be qualified due to the increasing effect of noise for increasingly weaker events.

Recently many works concerning ultraviolet brightenings in the quiet Sun atmosphere have been published and may give new insights into the coronal heating. However, the different data used and the pecularities of each analysis makes a direct comparison difficult. For example, Krucker et al. (1997) detected flare-like events, called network flares, using SXT on Yohkoh and the Very Large Array (VLA). Harrison (1997) reported on blinkers using CDS on SOHO. Berghmans et al. (1998) found good indications that the He II band brightenings and blinkers are compatible. They also identified coronal brightenings seen in an Fe XII line with X-ray network flares. The EUV explosive events, first detected by Brueckner & Bartoe (1983) using the HRTS instrument and then confirmed by Innes et al. (1997) using SUMER on SOHO, are high-velocity events originating from transition region lines. Until now it is not clear if and how explosive events and blinkers are related. Nor is it clear if the "high variability" events which we see in the O V and Mg IX lines are related to blinkers or network flares. Searching for such a connection will be the subject of a separate paper.

Acknowledgements. We would like to thank the CDS team, as well as the SOHO commanding staff whose help was invaluable in obtaining these observations. SOHO is a mission of international cooperation between ESA and NASA. This work was partly supported by the Swiss National Science Foundation, grant No. 21-45083.95, and by a grant from the ETH-Zürich which is greatly acknowledged.

References

Andretta V., Jones H.P., 1997, Apj 489, 375
Benz A.O., Krucker S., 1998, Solar Phys. 182, 349
Berghmans D., Clette F., Moses D., 1998, A&A 336, 1039
Brekke P., Kjeldseth–Moe O., Brynildsen N., et al. 1997, Solar Phys. 170, 163
Brueckner G.E., Bartoe J.-D.F., 1983, Apj 272, 329
Dere K.P., Landi E., Mason H.E., Monsignori Fossi B.C., Young P.R., 1997, A&AS 125, 149
Fontenla J.M., Avrett E.H., Loeser R., 1993, Apj 406, 319
Gallagher P.T., Phillips K.J.H., Harra–Murnion L.K., Keenan F.P., 1998, A&A 335, 733
Harrison R.A., Sawyer E.C., Carter M.K., et al., 1995, Solar Phys. 162, 233
Harrison R.A., 1997, Solar Phys. 175, 467
Huber M.C.E., Foukal P.V., Noyes R.W., et al., 1974, Apj 194, L115
Innes D.E., Inhester B., Axford W.I., Wilhelm K., 1997, Nat. 386, 811
Krucker S., Benz A.O., Bastian T.S., Acton L.W., 1997, Apj 488, 499
Landi E., Landini M., Dere K.P., Young P.R., Mason H.E., 1999, A&AS 135, 339
Lemaire P., Wilhelm K., Curdt W., et al., 1997, Solar Phys. 170, 105
Lin R.P., Schwartz R.A., Kane S.R., Pelling R.M., Hurley K.C., 1984, Apj 283, 421
Lites B.W., Hansen E.R., 1977, Solar Phys. 55, 347
Parker E.N., 1988, Apj 330, 474
Pauluhn A., Rüedi I., Solanki S.K., et al., 1999, Appl. Opt. 38, 34
Porter J.G., Toomre J., Gebbie K.B., 1984, Apj 283, 879
Rabin D., Dowdy J.F., 1992, Apj 398, 665
Reeves E.M., Vernazza J.E., Withbroe G.L., 1976, Phil. Trans. R. Soc. London, Ser. A 281, 319
Rüedi I., Brković A., Solanki S.K., et al., 1997, in: Proc. Fifth SOHO Workshop, 'The Corona and Solar Wind near Minimum Activity', A. Wilson (Ed.) ESA SP–404, 641
Schadee A., De Jager C., Švestka Z., 1983, Solar Phys. 89, 287
Shimizu T., Tsuneta S., Acton L.W., Lemen J.R., Uchida Y., 1992, PASJ 44, 147
Strong K.T., Harvey K., Hirayama T., et al., 1992, PASJ 44, 161

Thompson W., 1998, CDS Software Note # 49, Version 4, http://orpheus.nascom.nasa.gov/cds/software_notes.html
Ulmschneider P., Priest E.R., Rosner R. (Eds.), 1991, Mechanisms of Chromospheric and Coronal Heating, Springer-Verlag, Berlin
Vernazza J.E., Foukal P.V., Huber M.C.E., et al., 1975, Apj 199, L123
Walsh R.W., Ireland J., Harrison R.A., Priest E.R., 1997, Proc. Fifth SOHO Workshop, The Corona and Solar Wind near Minimum Activity, A. Wilson (Ed.) ESA SP–404, 717